Paper No.
61—WA-112

Cavitation in Turbo Pumps—Part 1

I. R. STRIPLING
Senior Research Engineer,
Rocketdyne Corporation,
Canoga Park, Calif.

A. J. ACOSTA
Associate Professor
of Mechanical Engineering,
California Institute of Technology,
Pasadena, Calif. Assoc. Mem. ASME

A free-streamline flow through a cascade of semi-infinite flat plates is taken as a simplified model of the cavitation process in a helical inducer pump. The length and thickness of the resulting cavity is determined as a function of blade geometry and cavitation parameter. Loss coefficients resulting from the cavitation are estimated and representative cavity shapes are calculated to aid in designing the leading edge shape of the blades.

Introduction

In recent years an increasing amount of attention has been devoted to problems of high-speed pumping systems. This has been brought about largely by the problems of developing lightweight turbomachine components for liquid-rocket propulsion systems. The weight of rotating equipment such as pumps and turbines for given power levels is, of course, reduced rapidly as the rotative speed is increased. The speed cannot be increased indefinitely, however, since the cavitation which develops in the inlet portions of the pump impeller limits the performance. The size and weight advantage conferred by higher rotative speeds is not limited to missile-pump applications. It is, in fact, always desirable to operate a liquid pumping system at the highest speed possible, subject only to the afore-mentioned limitations of cavitation. This is true for pumping applications in the petroleum industry as well as, for example, hydroelectric power-plant installations. The deterioration in performance caused by cavitation may occur in several ways. Extensive cavitation in the eye or inlet of the pump may give rise to appreciable mixing losses and therefore a reduced and possibly unacceptably low efficiency. The presence of the cavitation may also distort the flow pattern to such a degree that insufficient power is transmitted to the flowing fluid. Damage to the structure from the collapsing cavity voids either from erosion or vibration can also occur, but this is not the subject of present concern.

A knowledge of the conditions under which rapid deterioration of performance takes place by cavitation is therefore extremely important to the designer of all kinds of rotating equipment. In this paper we are concerned chiefly with the effects of cavitation in what are called "inducer pumps." Experience and theory both have shown that the inlet portions of the impeller must have a low blade angle and moderately high solidity[1] to forestall the effects of cavitation. These requirements usually result in a predominantly axial portion of the impeller entrance as shown in Fig. 1. (This portion may or may not be integral with the rest of the pump impeller.) The development of cavitation in such a device as the pressure is gradually lowered is quite complex [1].[2] For example, the flow is not usually steady nor is it always symmetric, i.e., the amount of cavitation may vary from blade to blade. Also, at moderate angles of attack complicated back flows, real fluid effects, and tip clearance cavitation confuse and obfuscate the observer. Some of these effects are illustrated in Fig. 2 in which the appearance of the cavitation is shown for various cavitation numbers and angles of attack on a helical inducer of constant pitch. With reduction in inlet pressure the cavitating region grows and moves downstream well into the passages of the inducer [1] and approaches the condition of the sudden decrease in performance (shown in Fig. 3) known as cavitation breakdown. Needless to say, it is of the utmost importance that the designer be able to estimate when this condition may take place.

Several papers have appeared in recent years that treat this problem. One of the first of these is due to Gongwer [2]. In this he adopted the model of a free-streamline flow through a cascade of flat plate hydrofoils due to Betz and Petersohn [3] to represent the cavity flow in the inlet of a centrifugal impeller. These same ideas were then later applied to cavitation in an axial inducer [1, 4] where the assumption of a planar cascade flow is more applicable than it is in a centrifugal impeller. It was observed in a study of helical inducers of constant pitch [1] that the minimum cavitation number that could be safely achieved was something like twice the value of that obtained from the free streamline theory of Betz-Petersohn, although due to the limitations of the experimental equipment, these results were not conclusive. Similar results were also found by other workers at about the same time.[3]

Contributed by the Hydraulic Division for presentation at the Winter Annual Meeting, New York, N. Y., November 26–December 1, 1961, of The American Society of Mechanical Engineers. Manuscript received at ASME Headquarters, July 27, 1961. Paper No. 61—WA-112.

[1] See notations.
[2] Numbers in brackets designate References at end of paper.
[3] T. Iura, private communication.

Nomenclature

c = length of cavity
$D = 2\pi$ = blade spacing
F = complex velocity potential $\bar{\varphi} + i\bar{\psi}$
$h = Y$ = wake or cavity height at cavity closure
$i = \sqrt{-1}$
k = cavitation number $(p_1 - p_c)/\rho w_1^2/2$
p = static pressure
P = total pressure
u = velocity component in x-direction
U_1 = impeller speed $w_1 \sin(\gamma + \alpha)$
v = velocity component in y-direction
w = magnitude of velocity vector
x, y = co-ordinates in physical plane
$z = x + iy$
α = angle of attack to blade
β = blade angle, $(\pi/2) - \gamma$
γ = stagger angle
ζ = hodograph variable $u - iv$
ρ = density (slugs/ft^3)
τ = cavitation parameter $(P_1 - p_c)/\rho U_1^2/2$
$\bar{\varphi}$ = velocity potential
$\bar{\psi}$ = stream function
ψ = head coefficient, total pressure increase across rotor/ρU_1^2
ψ_f = total pressure loss coefficient $(P_1 - P_3)/\rho U_1^2$

Subscripts

1 = far upstream of cascade
2 = far downstream of cascade (within passage)
3 = after mixing process far downstream
c = quantities evaluated on free streamline

Discussion on this paper will be accepted at ASME Headquarters until January 10, 1962

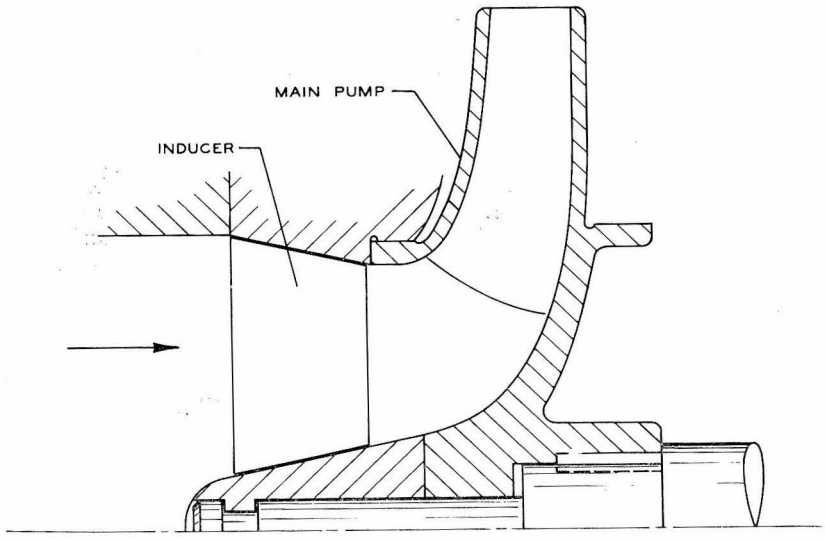

Fig. 1 Cross section of typical pump-inducer combination

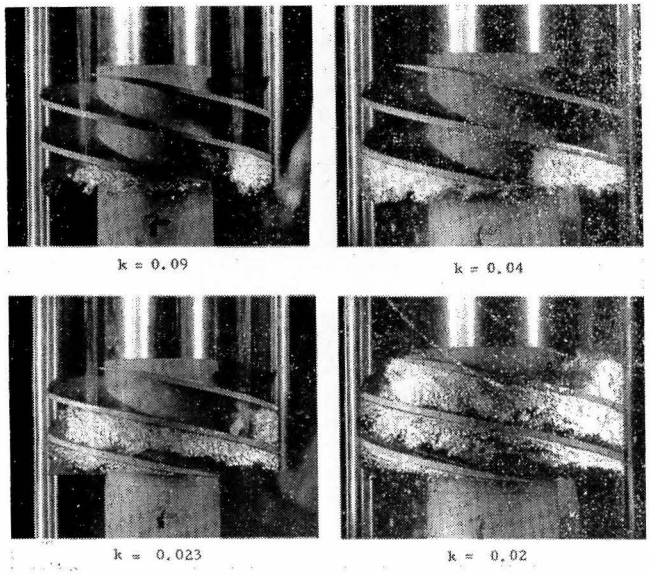

Fig. 2(a) Development of cavitation in a helical inducer with a 12-deg tip angle at a flow coefficient of $\varphi = 0.12$ (the average axial velocity divided by the impeller tip speed) for various cavitation numbers. Performance is seriously reduced in the lower right photograph.

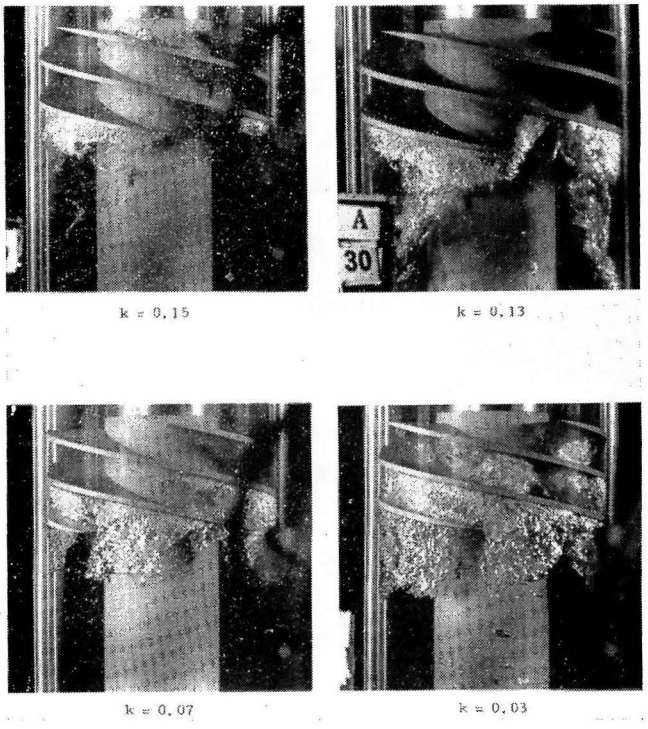

Fig. 2(b) Cavitation development at a flow coefficient of $\varphi = 0.08$ in a 12-deg inducer for various cavitation numbers

The assumption of planar flow along cylindrical sections through an inducer is, of course, a great simplification. Radial flows are developed along the constant pressure surfaces of the cavity (which are themselves primarily radial), and the axial velocity distribution through the inducer, which depends upon the radial work distribution of the rotor, is rarely constant, for inducer pumps are seldom free vortex designs [5]. In addition, observations and rough calculations [1, 6] show that appreciable radial boundary-layer flows take place along the surfaces of the blades. Nevertheless, the free streamline theory appears to be a good guide in determining the cavitation limits of these simplified pumping configurations and more especially is it useful as a basis for correlating experimental tests.

The remainder of the present paper discusses several simplified free streamline models suitable for the flow through an inducer and in a companion paper[4] these results are compared with tests on actual inducers. It will be shown that, with the use of experimentally determined correlating factors, this theory forms a useful basis of design. The present studies are limited to helical inducers of large solidity constant pitch and constant hub and tip radii for simplicity. Furthermore, it is assumed that the cavitation phenomenon in such flows is well represented by a free-streamline model and that the vapor pressure within the cavity is

[4] L. B. Stripling, "Cavitation in Turbo Pumps—Part 2," ASME Paper No. 61—WA-98.

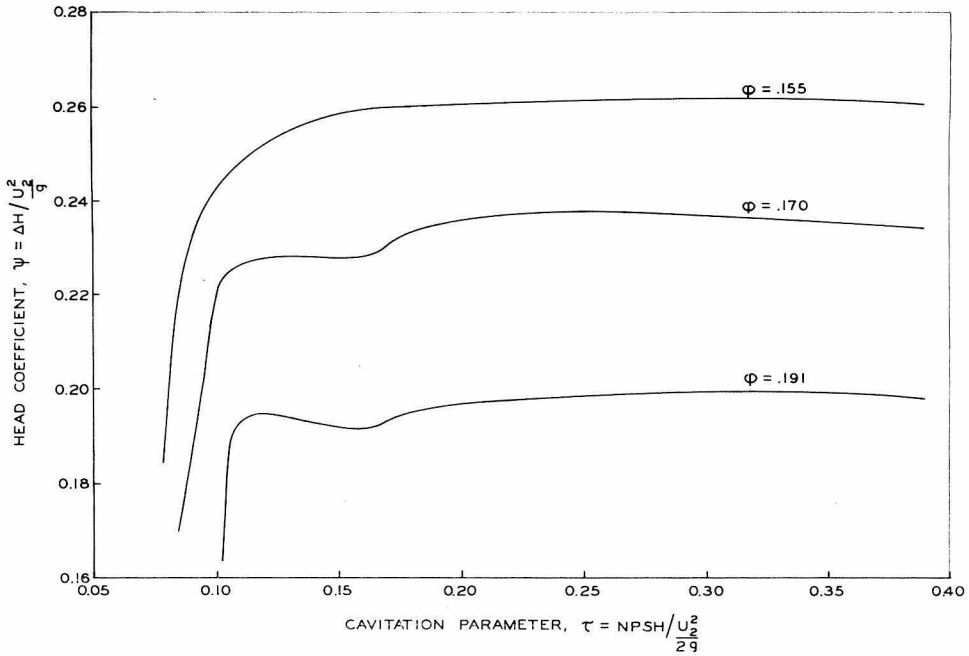

Fig. 3 Typical performance of an inducer pump with 18-deg tip angle, 0.31 hub ratio and 1.25 tip solidity (chord over circumferential blade spacing). (φ is the axial velocity divided by impeller tip speed which is here denoted by U_2.)

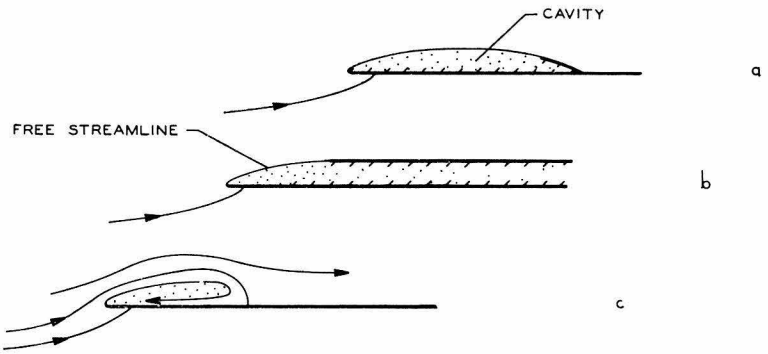

Fig. 4 Sketch of various cavitation models: (a) Image plate; (b) "transition" or wake model; (c) re-entrant jet

known. These latter conditions may not be fulfilled, especially for some of the cryogenic fluids now in common use. Here, allowance must be made for the so-called "thermal effect" [7] and possibly for the existence of other modes of cavitation such as the foaming that takes place when liquid hydrogen cavitates[5] rather than a distinct cavity as is presumed below. These considerations, however, are beyond the scope of the present article.

Cavitation Models

The model we take for the flow is that of a series of flat plate hydrofoils arranged in an infinite cascade with a free streamline originating from the leading edge of each hydrofoil. The flow is assumed to be two-dimensional, irrotational, and inviscid. The cavity may be longer than the chord of the hydrofoil but observations [1] have shown that, to provide the necessary flow turning, the cavity must lie within the blade passage. There is no unique solution for a constant pressure cavity of finite length, as there are a variety of ways in which the cavity can be terminated (see, for example, the book by Birkhoff and Zarantonello [8]). Among these are a re-entrant jet, an image plate on which the free streamline collapses, or the free streamline may gradually recover pressure on a solid boundary that resembles a wake. These are sketched in Fig. 4. While all of these various models give more or less the same numerical results, it is believed that the wake model (sometimes called the "dissipation" model) simulates to some degree the actual wake downstream of the cavity terminus where intense mixing is observed to occur. This is not particularly important for flows over isolated hydrofoils, but when the flow is confined, as it is in a cascade or water tunnel, the blockage of the wake is important in determining the subsequent downstream flow. The actual wake thickness and structure of the real flow cannot, of course, be determined from a perfect fluid theory, so that there is considerable arbitrariness in any particular mathematical model chosen for the flow. Therefore, we will take the simplest possible model that retains the desired features mentioned above.

It was mentioned that an inducer operates with the cavitation bubble or region within the blade passage. That is, the length of the cavity is less than the chord, so that we are interested primarily in the case of "partial" cavitation. Since the chord of an

[5] Private communication, W. Wilcox, NASA, Cleveland, Ohio.

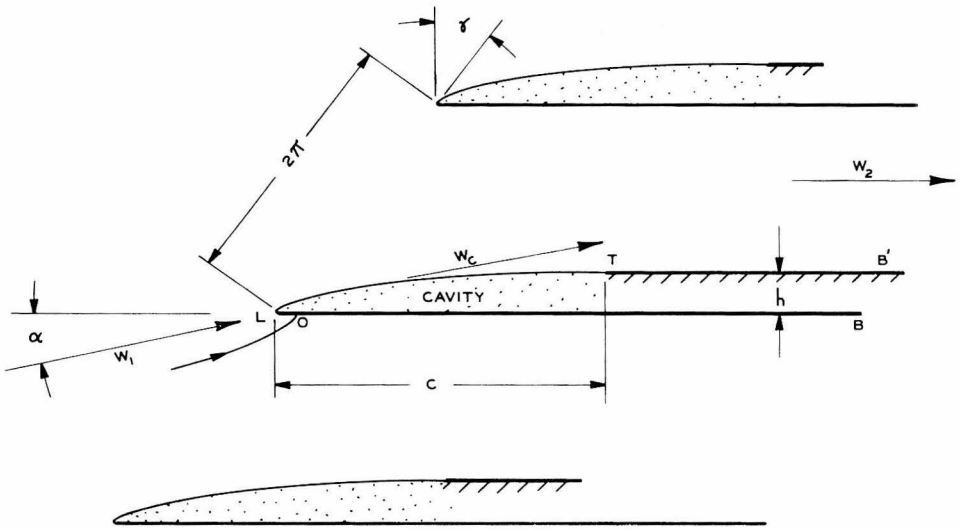

Fig. 5 Sketch of partly cavitating cascade

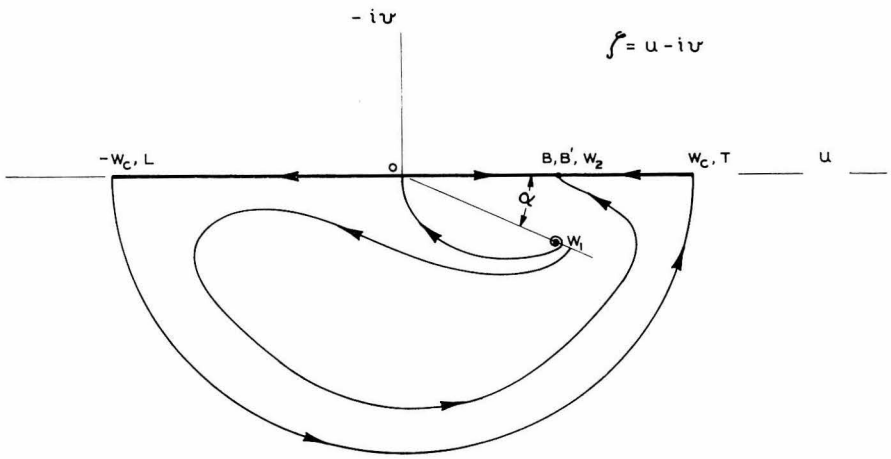

Fig. 6 Hodograph of the flow in the physical plane

inducer pump is ordinarily much longer than the peripheral spacing (say, two or three times) we will simplify the work below by taking the chord to be infinitely long and studying the development of the cavity in the inlet region as the pressure is lowered.[6]

Formulation of Problem

An upstream flow of uniform velocity w_1 approaches the staggered array of flat plates at an angle α as shown in Fig. 5. A free streamline originates at the leading edge of each plate and closes upon a flat surface parallel to the original surface. The length of the cavitating region c as well as its height h are to be determined as functions of the stagger angle γ, angle of attack α, and the cavitation number k which relates the upstream velocity w_1 to the velocity along the constant pressure surface w_c. The cavitation number for this flow is defined to be

$$k = \frac{p_1 - p_c}{\rho w_1^2/2} \tag{1a}$$

and from the Bernoulli relation

$$w_c = w_1\sqrt{1 + k} \tag{1b}$$

As is customary in problems involving free streamlines, it is convenient to discuss the flow in reference to the hodograph plane, in which the streamlines that describe the wetted surfaces and constant pressure surfaces are sketched as a function of the hodograph variable $\zeta = u - iv$. That is, if $F = \tilde{\varphi} + i\tilde{\psi}$ is the complex potential of the flow, with $\tilde{\varphi}$ being the velocity potential and $\tilde{\psi}$ the stream function, then

$$\zeta = \frac{dF}{dz} = u - iv \tag{2}$$

where u, v are the x and y-velocity components in the physical plane, and $z = x + iy$ is the complex variable in the physical plane. The solution rests upon the fact that the imaginary part of F is known around the boundary of the flow as seen in the hodograph plane. This is shown in Fig. 6 and corresponding points in the physical and hodograph plane are identified. If F

[6] The case of finite chord length has also been worked out but no computations have been made. See also G. A. Dombrovsky, "On Free Streamline Flow at Subsonic Velocities About an Infinite Lattice of Flat Plates," Doklady Academy Nauk USSR, 1956, vol. III, no. 2, p. 312. Translated by G. and H. Cohen, Rensselaer Polytechnic Institute, RPI Trans. no. 3.

can be determined as a function of ζ, then physical co-ordinates for corresponding points in the ζ-plane can be determined by integrating (2), i.e.,

$$z = \int \frac{dF}{\zeta} + \text{const} \tag{3}$$

The usual procedure to determine $F(\zeta)$ is to transform the hodograph onto the potential plane $F = \bar{\varphi} + i\bar{\psi}$ by suitable intermediate steps. In the present work, however, the hodograph is sufficiently simple so that the solution $F(\zeta)$ can be determined by inspection as was done in the original work of Betz and Petersohn.

This is greatly facilitated by recognizing that the uniform flows at infinity correspond to source-vortexes located at their corresponding points in the hodograph plane. For example,

$$F = w_1 e^{-i(\alpha+\gamma)} \ln (\zeta - w_1 e^{-i\alpha})$$

represents a source-vortex in the ζ-plane located at the point corresponding to $z = -\infty$. Then, from (3), the corresponding physical co-ordinates are

$$z = w_1 e^{-i(\alpha+\gamma)} \int \frac{d\zeta/\zeta}{\zeta - w_1 e^{-i\alpha}} = e^{-i\gamma} \ln [(\zeta - w_1 e^{-i\alpha})/\zeta] + \text{const}$$

When $w_1 e^{-i\alpha}$ is encircled once in the counterclockwise direction, z moves a distance 2π to a corresponding point on the next step of the cascade. (The slant height of the cascade can be changed to any other value by introducing a scale factor.) Also it is readily shown that the streamlines in the ζ-plane near the origin of the vortex are uniform and inclined at the angle α to the x-axis in the physical plane.

Solution

The complex potential must have the appropriate singular behavior indicated above at each of the points $-\infty$, $+\infty$ of Fig. 6. In addition the real axis and the circle $|\zeta| = w_c$ must be streamlines in the hodograph. Finally, it is necessary that the point $\zeta = 0$ be a stagnation point of this flow which requires that

$$\frac{dF}{d\zeta}(\zeta = 0) = 0. \tag{4}$$

The potential satisfying the above conditions, determined by the method of images, is

$$\begin{aligned}\frac{1}{w_1} F(\zeta) &= e^{-i(\gamma+\alpha)} \ln (\zeta - w_1 e^{-i\alpha}) \\ &+ e^{i(\gamma+\alpha)} \ln (\zeta - w_1 e^{i\alpha}) + e^{i(\gamma+\alpha)} \ln \left(\zeta - \frac{w_c^2}{w_1} e^{-i\alpha}\right) \\ &+ e^{-i(\gamma+\alpha)} \ln \left(\zeta - \frac{w_c^2}{w_1} e^{i\alpha}\right) - 2 \cos (\gamma + \alpha) \\ &\left[\ln (\zeta - w_2) + \ln \left(\zeta - \frac{w_c^2}{w_2}\right)\right] + \text{const}\end{aligned} \tag{5}$$

and in order that (4) be fulfilled the following relationship between the velocity ratios must hold:

$$\frac{w_c}{w_2} + \frac{w_2}{w_c} = \left(\frac{w_c}{w_1} + \frac{w_1}{w_c}\right) \cos \alpha + \left(\frac{w_c}{w_1} - \frac{w_1}{w_c}\right) \sin \alpha \tan (\gamma + \alpha) \tag{6}$$

It is interesting to observe that (6) can be derived from momentum considerations alone, so that this relationship merely states that the force on the hydrofoils is normal to the chord.

The physical co-ordinates of the flow, obtained by integrating (3), are

$$\begin{aligned}z &= e^{-i\gamma} \ln (\zeta - w_1 e^{-i\alpha}) + e^{i\gamma} \ln (\zeta - w_1 e^{i\gamma}) \\ &+ \frac{w_1^2}{w_c^2} e^{i(\gamma+2\alpha)} \ln \left(\zeta - \frac{w_c^2}{w_1} e^{-i\alpha}\right) \\ &+ \frac{w_1^2}{w_c^2} e^{-i(\gamma+2\alpha)} \ln \left(\zeta - \frac{w_c^2}{w_1} e^{i\alpha}\right) \\ &- 2 \frac{w_1}{w_2} \cos (\gamma + \alpha) \left[\ln (\zeta - w_2) + \frac{w_2^2}{w_{c2}} \ln \left(\zeta - \frac{w_c^2}{w_2}\right)\right] + \text{const}\end{aligned} \tag{7}$$

Our primary interest is in the co-ordinates of the leading edge and terminus of the cavity. These are the length of the cavity c measured from the leading edge and the height of the wake measured normal to the blades. Upon reference to Fig. 5, it can be seen that the difference in these co-ordinates is given by

$$c + ih = z(\zeta = w_c) - z(\zeta = -w_c) \tag{8}$$

and to insure the correct branches of (7), the argument of ζ must increase from $-\pi$ to 0 as ζ increases from $-w_c$ along the circle $|\zeta| = w_c$. After some manipulation we obtain

$$h = 2\pi \cos \gamma \left[1 - \frac{w_1}{w_2} \frac{\cos (\gamma + \alpha)}{\cos \gamma}\right] \tag{9}$$

and

$$\begin{aligned}c &= \left(\cos \gamma + \frac{w_1^2}{w_c^2} \cos (\gamma + 2\alpha)\right) \ln \left(\frac{w_c^2 - 2w_1 \cos \alpha + w_1^2}{w_c^2 + 2w_1 \cos \alpha + w_1^2}\right) \\ &- 2 \cos (\gamma + \alpha) \left[\frac{w_1}{w_2} + \frac{w_1 w_2}{w_c^2}\right] \ln \frac{w_c - w_2}{w_c + w_2} \\ &+ 2 \left(\sin \gamma + \frac{w_1^2}{w_c^2} \sin (\gamma + 2\alpha)\right) \tan^{-1} \frac{2w_1 w_c \sin \alpha}{w_c^2 - w_1^2}\end{aligned} \tag{10}$$

The solution to the problem set out is summarized in equation (6), (9), and (10). For example, let γ, α, and k be given. w_c is then found from (1*b*) and w_2 from (6). h and c then follow immediately from (9) and (10), respectively.

Discussion

First, let us examine the two limiting cases $k \to \infty$ and $c \to \infty$. For the former case as $k \to \infty$, $w_c/w_1 \to \infty$ and we see from (6) that $w_1/w_2 \to \cos \gamma/\cos (\gamma + \alpha)$ so that both h and c approach zero. That is, the flow becomes fully wetted and the pressure at the leading edge becomes negatively infinite as it should. Thus, as k increases, c decreases. At the other extreme we note that if $w_c = w_2$, c or the cavity length becomes infinite. This corresponds to the Betz-Petersohn case for infinite chord length. The cavitation number is not zero for infinite cavity length but is given by (6) with $w_c = w_2 = w_1\sqrt{1 + k}$, and is the minimum value of k achievable in the cascade. Thus,

$$\underset{\text{min}}{k} = \frac{2 \sin \alpha \cos (\gamma + \alpha)}{1 + \sin \gamma} \tag{11}$$

Equation (11) brings out clearly that to obtain small cavitation numbers, γ should approach 90 deg. When $\alpha = 0$ or $\gamma + \alpha = \pi/2$ it is seen that $k_{\text{min}} = 0$ but these values are not realistic since in the first case blade thickness and boundary-layer blockage restrict the flow and, in the second, there is no net through flow. Between these extremes k_{min} achieves a maximum value (for γ const) when $\alpha = \pi/4 - \gamma/2$ of $(1 - \sin \gamma)/(1 + \sin \gamma)$. This shows again that large values of γ are necessary to obtain small values of k.

The results of the foregoing (albeit elementary) problems are

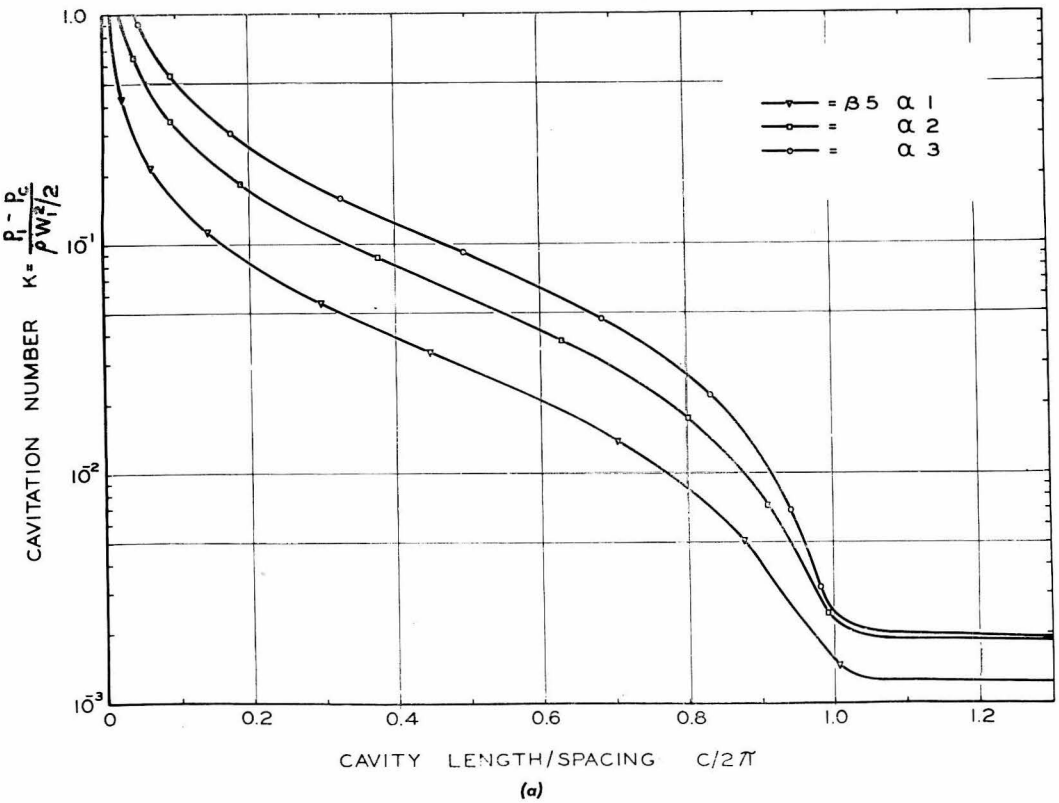

(a)

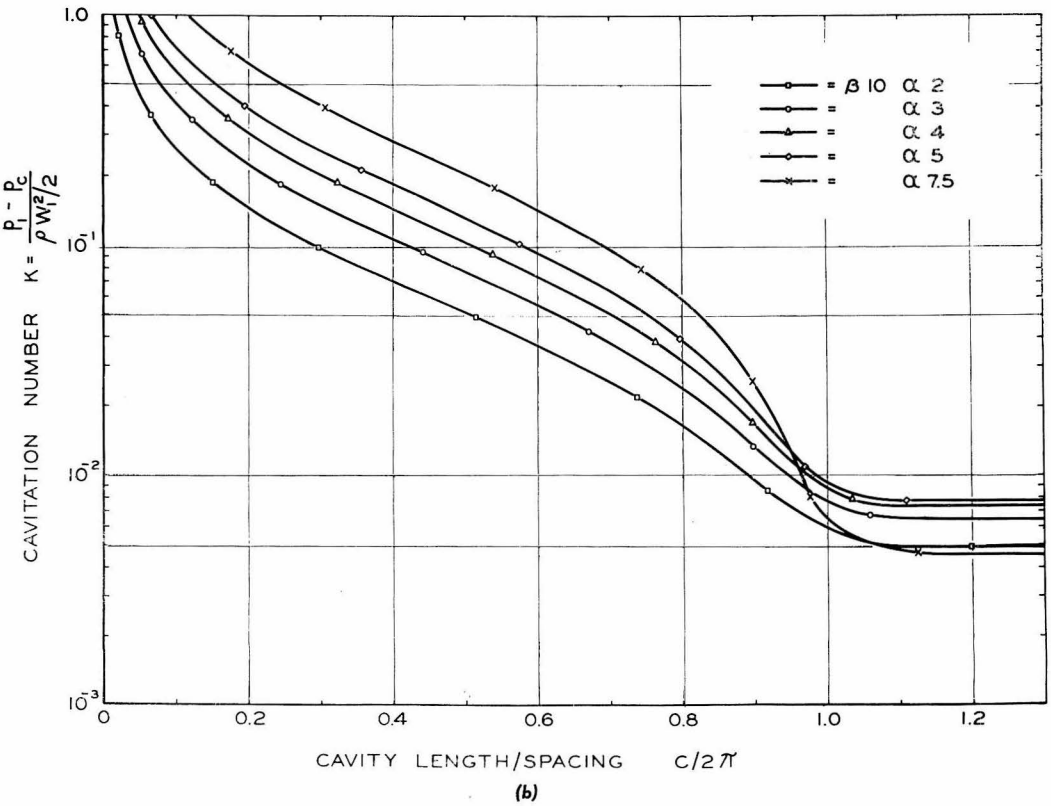

(b)

Fig. 7 Cavity length—spacing ratio versus cavitation number for various blade angles and angles of attack

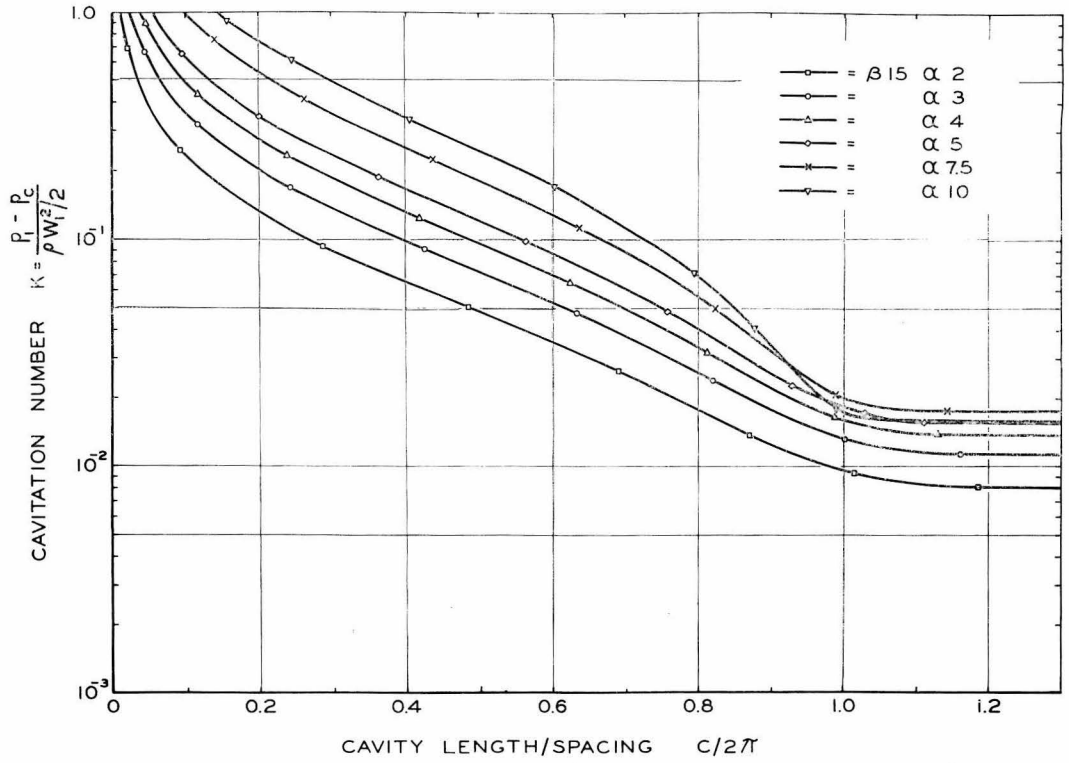

Fig. 7(c)

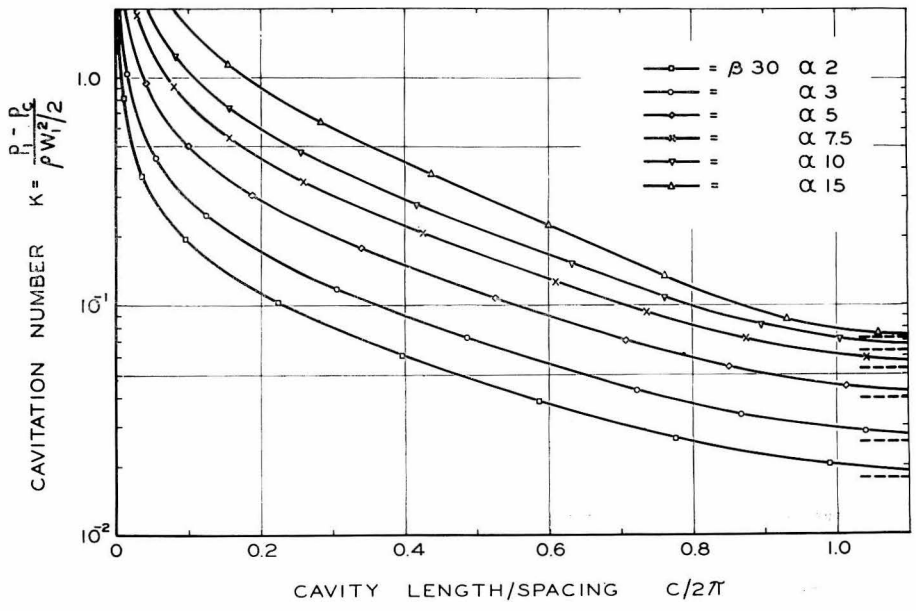

Fig. 7(d)

believed to be of some interest to pump designers. Therefore, extensive computations of the characteristics of this cascade flow have been carried out and are presented in Figs. 7 to 13. The first of these (Fig. 7) shows how the length of the cavity increases as the cavitation number is descreased for various inlet angles α and blade angles β (the complement of γ). It is of special interest to observe that the minimum cavitation number is achieved when the length-spacing ratio is about unity for all except the smallest blade angles. Since the blade chord to spacing ratio of most inducer configurations is about one and a half to two, we may take this result to mean that the assumption of infinite blade chord does not invalidate the results of the present calculations for practical configurations. In fact, it suggests that inducers of considerably lower solidity could be used to good effect.

The cavitation number is not particularly convenient for use in applications, however, so that the results of the foregoing have

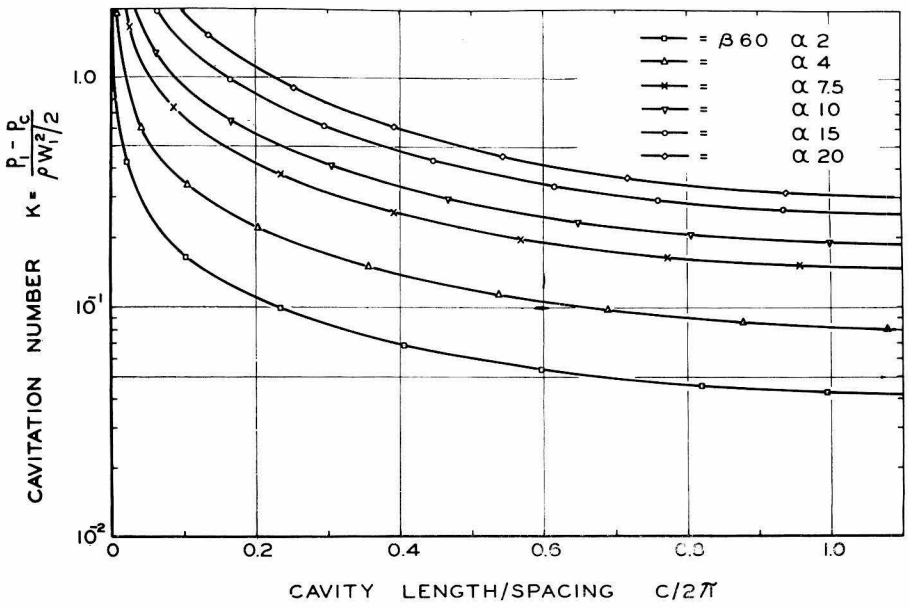

Fig. 7(e)

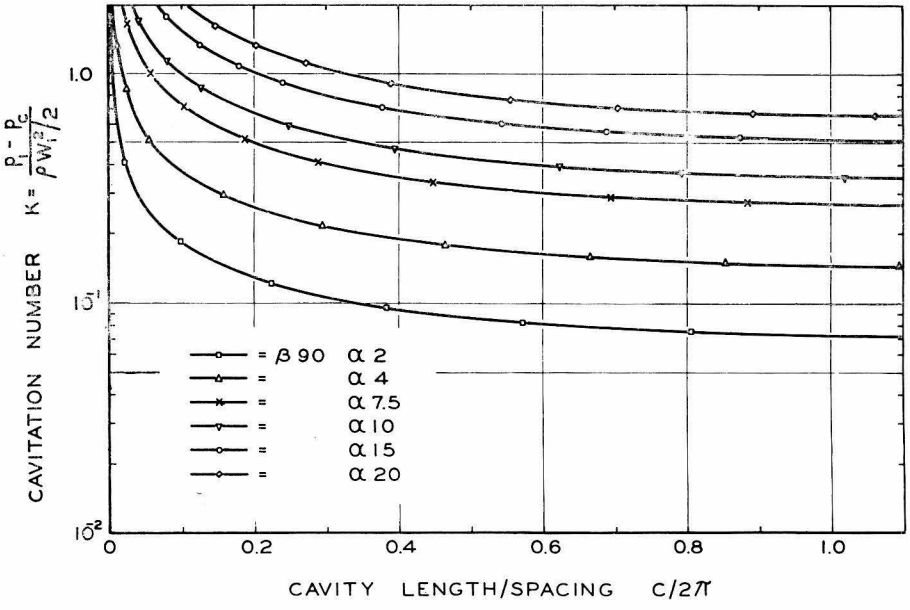

Fig. 7(f)

been presented in Fig. 8 in terms of an equivalent parameter.

$$\tau = \frac{\text{NPSH}}{U_1^2/2g} = \frac{P_1 - p_c}{\rho U_1^2/2} \tag{12}$$

where the abbreviation NPSH stands for the "net positive suction head" and U_1 is the speed of the inducer blade (no prerotation is assumed to occur). This parameter is of direct use in application since the NPSH and rotative speed of the pumping application are usually known in advance.

The height of the cavity compared to the blade spacing is shown in Fig. 9 for an angle of attack of four degrees as a function of the cavitation number. Note that these curves all terminate at the minimum cavitation number possible for the cascade at each particular blade angle and angle of attack. Also shown by the dotted lines are crossplots for chord spacing ratios of 0.5 and 1.0. It is interesting to observe that the maximum heights in each case are nearly reached when the cavity-spacing ratio is unity.

Some idea of the proportions of cavities is given in Fig. 10, again for an angle of attack of four degrees. For the most part, the cavities are rather "slender" except for large cavitation numbers, say, in excess of 0.25.

Mixing Loss

In the present model, the flow becomes asymptotically parallel to the blades, and because of the finite height of the cavity wake, it does not fill the passage. For all real cavity flows, however, the cavity collapses and fluid will completely occupy the region between the blade surfaces of the impeller. Again, in a real fluid,

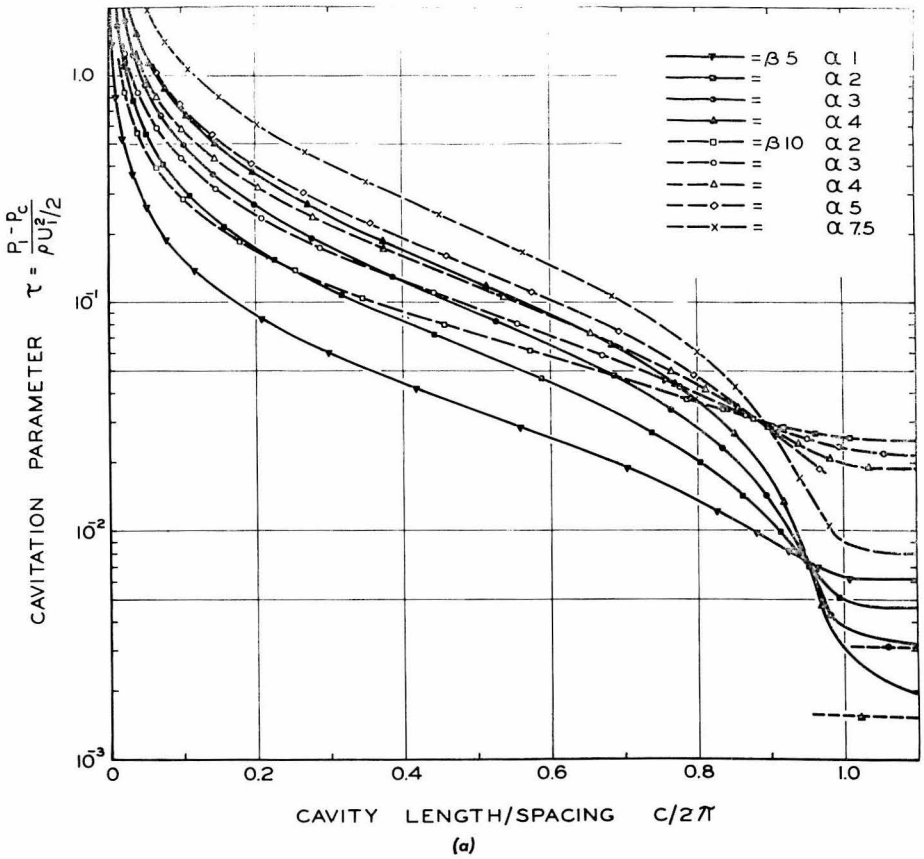

(a)

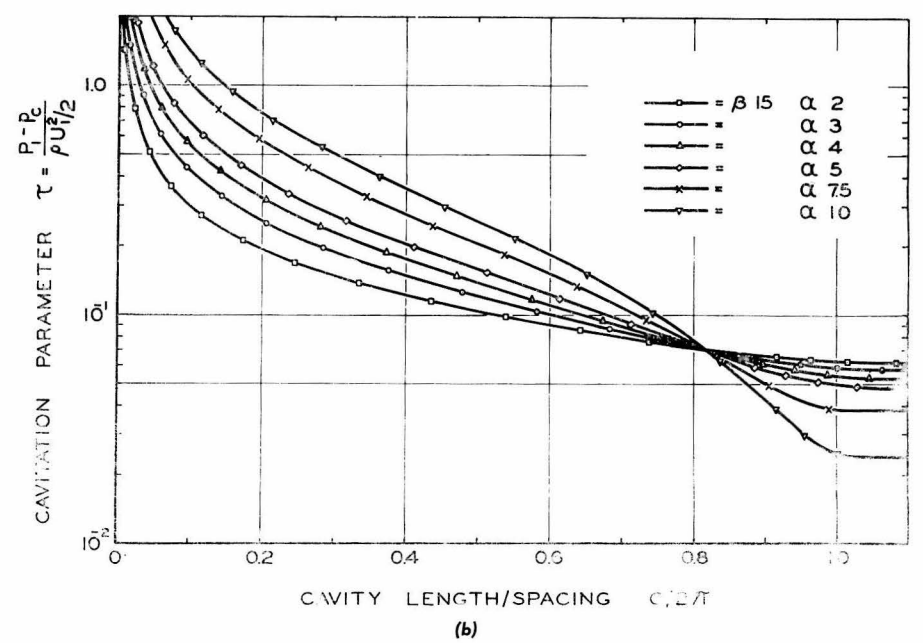

(b)

Fig. 8 Cavity length—spacing ratio versus cavitation parameter τ for various blade angles and angles of attack

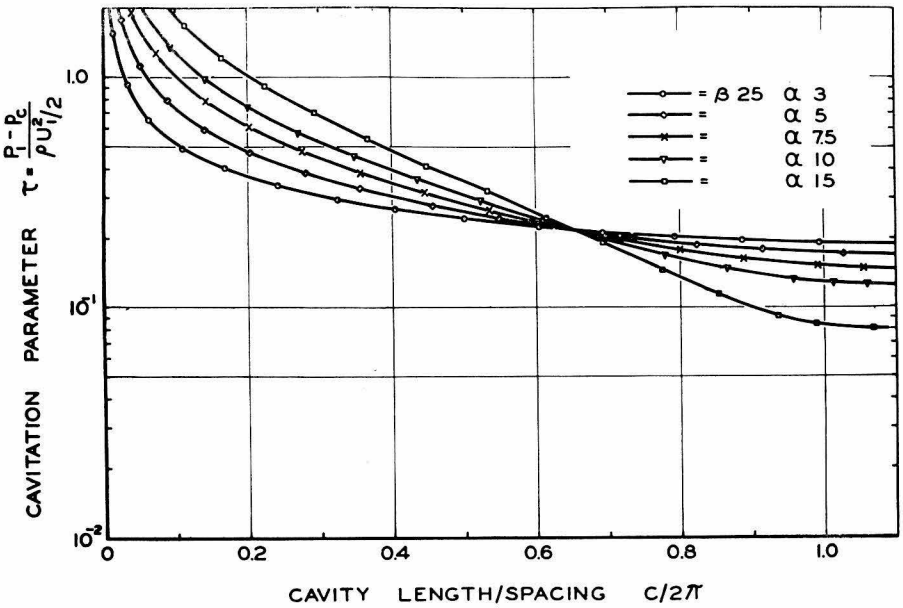

Fig. 8(c)

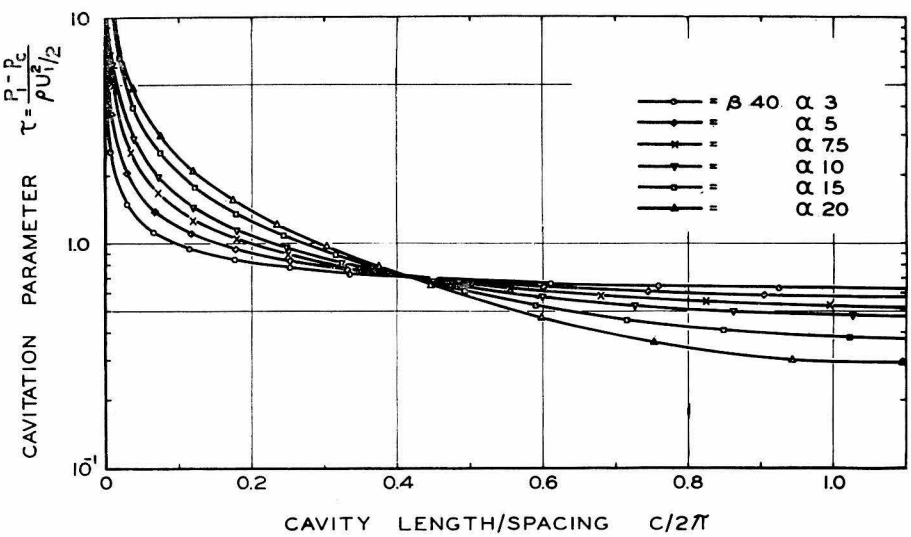

Fig. 8(d)

there will be a certain inherent mixing loss in this process which arises from destroying the momentum of the re-entrant jet that tends to form in cavity flows. This effect may be estimated from the present calculations by permitting the flow to undergo a rapid expansion to the full area between the blade passages. Thus, the head loss will be

$$h_f = \frac{(w_2 - w_3)^2}{2g}$$

where w_3 is obtained from the continuity equation

$$w_1 \cos(\gamma + \alpha) = w_3 \cos \gamma.$$

This relationship neglects the thickness of the blade and therefore tends to overestimate this loss. It is convenient to express the mixing loss in terms of the coefficient

$$\psi_f = gh_f/U_1^2 \tag{13}$$

for now ψ_f represents that part of the total head generated by the blade section under consideration that is lost due to cavitation. Of course, other more complicated real fluid and cavitation interactions may occur, but we are unable to estimate them with the present theory. Similar mixing losses are also reported for a fully cavitated, i.e., infinite cavities, cascade of finite flat plate hydrofoils by Cornell [9]. The present results, shown in Fig. 11 for an inlet angle of four degrees, therefore illustrate how the loss coefficient ψ_f varies with inlet pressure for a given cascade geometry. With this diagram at the special angle of attack listed rapid estimates of the total pressure loss due to cavitation alone can be made. The maximum loss $\psi_{f\,\max}$ is not much greater than that for the cavity length-spacing ratio of unity in conformity with the results of Fig. 9, so that the charts of Cornell's work

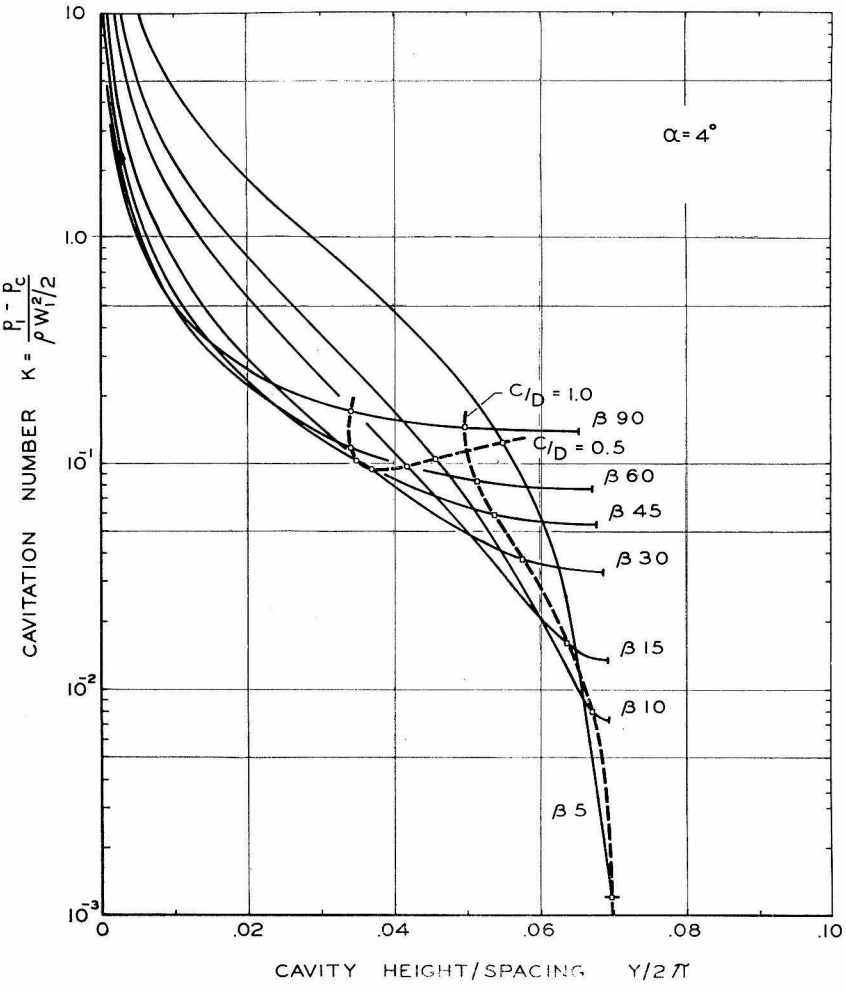

Fig. 9 Cavity height—spacing ratio versus cavitation number for an angle of attack of 4 deg. The symbol c/d stands for the length-spacing ratio.

can be used for this case as well. For reference we also include a plot of the maximum loss coefficient $\psi_{f\ max}$ as a function of inlet angle, Fig. 12.

Cavity Shape

To realize the cavitation performance of the present calculations, it is necessary that the suction side of the blade not interfere with the free streamline. This is particularly important near the leading edge where the cavity may be quite thin. Representative free streamlines were therefore calculated for a blade angle of 15 and 6-deg angle of attack, utilizing equation (7). The leading edge of the blade should therefore be filed so that it will not contact the free streamline. This requires, especially for the lower cavitation number of Fig. 13, a rather pointed leading edge contour. If the blade shape is blunter than the free streamline shape for the desired operating cavitation number, a drag force parallel to the blade chord will be experienced. This will have the undesirable result of increasing the mixing loss and the minimum cavitation number for the cascade. In practice[7] blunt leading edge shapes have inferior cavitation performance to slender shapes, and those that have the pressure side of the blade filed are inferior to those with the suction side filed in conformance to the above ideas.

[7] See part 2 of the present paper.

Acknowledgments

This work was supported by the Office of Naval Research Contract Nonr-220(24) and the Rocketdyne Division of North American Aviation, Inc. Reproduction for any purpose of the United States Government is permitted.

References

1 A. J. Acosta, "Experimental Study of Cavitating Inducers," Second Symposium on Naval Hydrodynamics, August, 1958, Washington, D. C.

2 C. A. Gongwer, "A Theory of Cavitation Flow in Centrifugal Pump Impellers," TRANS. ASME, vol. 63, 1941, pp. 29–40.

3 A. Betz and E. Petersohn, "Anwendung du Theorie der Frien Strahlen," Ing. Archiv., Band II, 1931.

4 A. J. Acosta and A. Hollander, "Remarks on Cavitation in Turbomachines," Engineering Division Report E-79.3, California Institute of Technology, Pasadena, Calif., October, 1959.

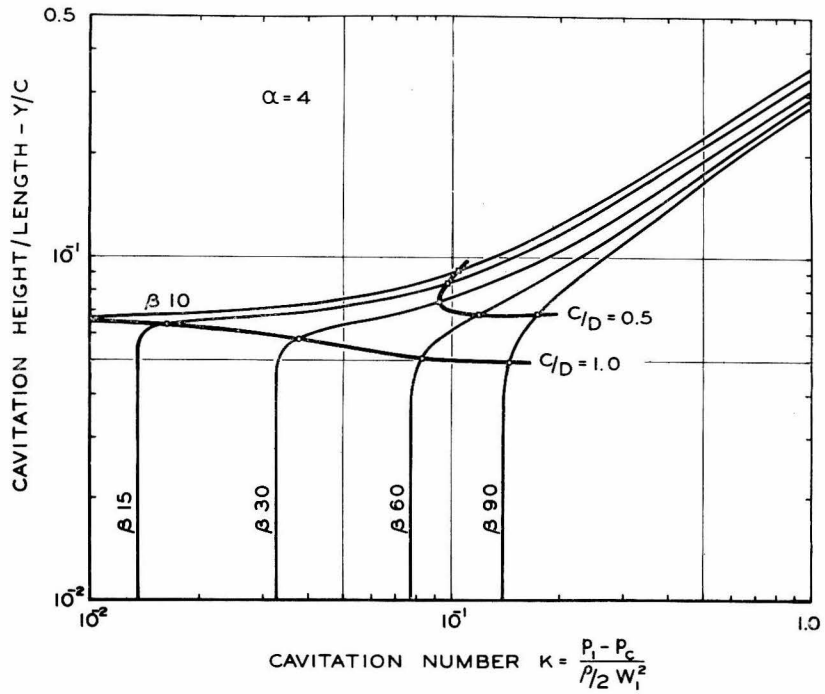

Fig. 10 Cavity height—length ratio versus cavitation number for an angle of attack of 4 deg. The symbol c/d represents the length-spacing ratio.

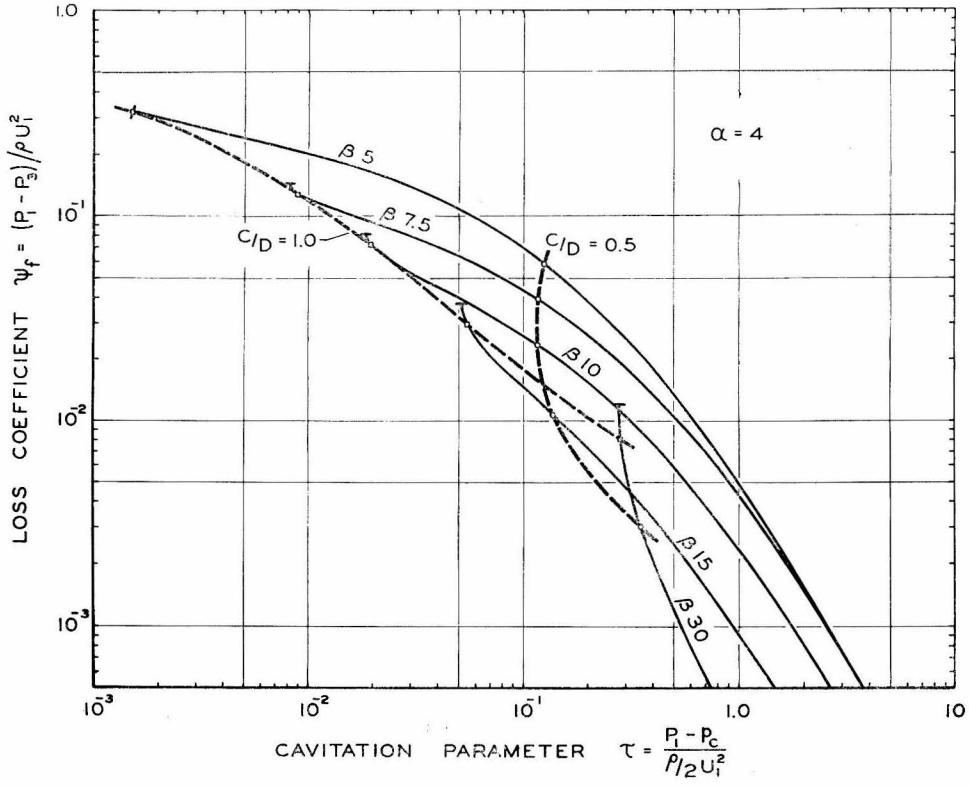

Fig. 11 Loss coefficient versus cavitation parameter τ for an angle of attack of 4 deg and various blade angles

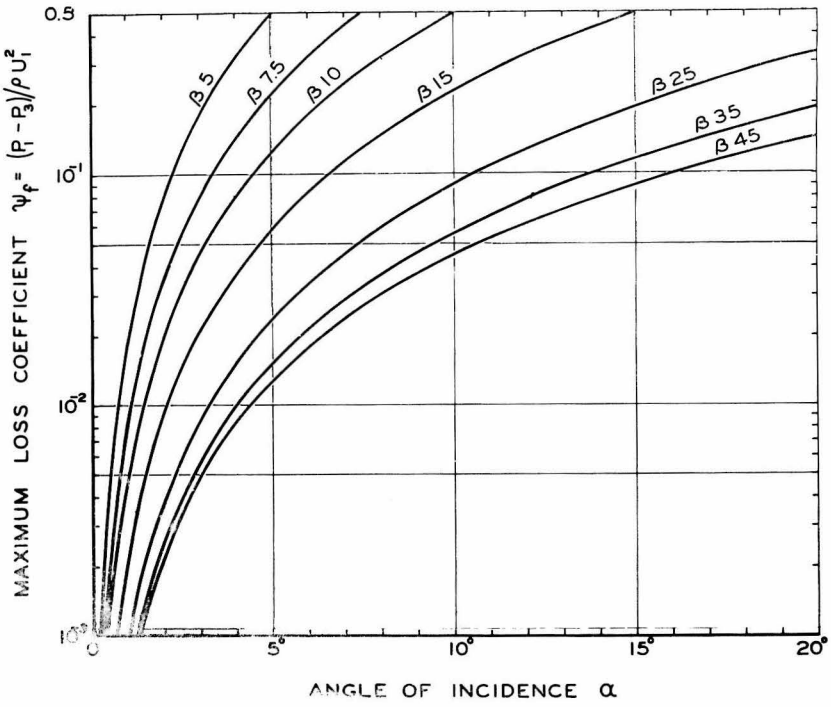

Fig. 12 Maximum loss coefficient versus angle of attack or incidence for various blade angles

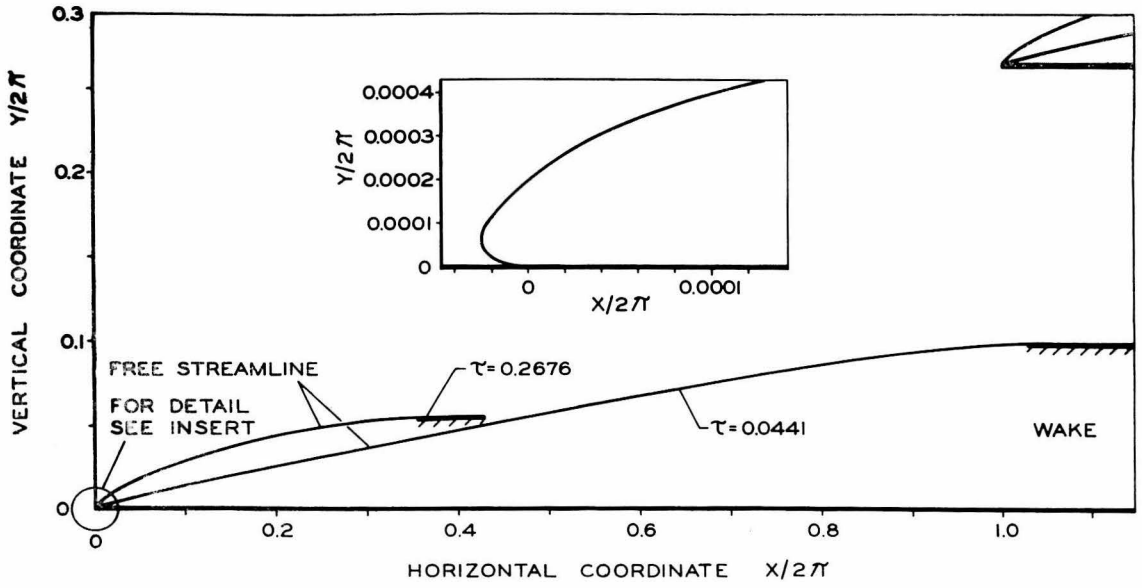

Fig. 13 Cavity shape for two cavitation numbers for a blade angle of 15 deg and an angle of attack of 6 deg. (Note the distorted scale.)

5 J. C. Montgomery, "Analytical Performance Characteristics and Outlet Flow Conditions of Constant and Variable Lead Helical Inducers for Cryogenic Pumps," NASA TN D-583.

6 A. J. Acosta, and G. F. Wislicenus, "Some Comments on Pump Cavitation Research," WADD Tech. Note 60-23.

7 V. Salemann, "Cavitation and NPSH Requirements of Various Liquids," JOURNAL OF BASIC ENGINEERING, TRANS. ASME, Series D, vol. 81, 1959, pp. 167–173.

8 G. Birkhoff and E. Zarantonello, "Jets, Wakes, and Cavities," Academic Press, 1957.

9 W. Cornell, "The Stall Performance of Cascades," Proceedings, Second National Congress of Applied Mechanics, June, 1954.

Printed in U. S. A.